

Enhanced Binding of Altered H-NS Protein to Flagellar Rotor Protein FliG Causes Increased Flagellar Rotational Speed and Hypermotility in *Escherichia coli**

(Received for publication, June 1, 1998, and in revised form, June 29, 1998)

Gina M. Donato and Thomas H. Kawula‡

From the Department of Microbiology and Immunology, University of North Carolina School of Medicine, Chapel Hill, North Carolina 27599-7290

H-NS is an *Escherichia coli* nucleoid protein known only to function as a modulator of gene expression. In this study, we found that specific single amino acid substitutions in H-NS caused an approximately 50% increase in flagellum rotational speed. In fluorescence anisotropy and chemical cross-linking assays, H-NS interacted with the flagellar torque-generating rotor protein FliG to form a complex with a K_d of 2.15 μM . Furthermore, one of the altered H-NS proteins that exhibited high speed flagellum rotation bound FliG 50% tighter than wild-type H-NS. These results demonstrate the first non-regulatory role for H-NS and provide a direct correlation between H-NS-FliG binding affinities, flagellar rotation, and motor torque generation.

Motility in many bacterial species is achieved by rotating surface-exposed organelles called flagella. In *Escherichia coli* and *Salmonella typhimurium* about 50 genes are required for the biosynthesis and operation of these peritrichous, multicomponent structures. Gene expression is hierarchical, whereby one class of genes must be turned on before the next class can be expressed. At the top of this cascade lies the *flhCD* master operon, whose expression is required for the expression of all other flagellar genes (reviewed in Refs. 1 and 2).

Flagellar filament rotation is controlled by a motor embedded in the inner membrane (reviewed in Refs. 1 and 3). Energy to drive this motor is derived from the transmembrane gradient of protons, or proton-motive force (4, 5). Bacteria swim by a random walk consisting of a series of runs and tumbles (6). When the motor rotates counterclockwise (CCW),¹ flagella filaments form a tight bundle that propels the bacterium into a smooth swimming pattern. Conversely, during clockwise (CW) rotation, flagellar filaments separate, causing tumbling and directional reorientation (7).

The *E. coli* flagellar motor consists of a MotA-MotB stator complex which forms a transmembrane proton channel (8–10), and a rotor of three interacting proteins, FliG, FliM, and FliN (11, 12). All three rotor proteins are involved in the processes of flagellar assembly, switching, and rotation (13, 14). However, FliG is predominately involved in torque generation (12, 14, 15), whereas FliM mainly functions in switching rotor direction (16). The precise role of FliN is the least well defined, but it

may participate in flagella protein-specific export and assembly (17, 18).

It has been shown that *hns* insertion mutations render bacteria non-motile, suggesting that H-NS is a positive regulator of flagellar gene expression (19, 20). H-NS is a 15.4-kDa nucleoid-associated DNA-binding protein (21–23) that modulates the expression of many unrelated genes in *E. coli* (24–26). In most instances, such as *fimB* (27) and *proU* (28) expression, H-NS acts as a direct transcriptional repressor.

Here we characterized two independent *hns* point mutations, *hnsT108I* and *hnsA18E*, in relation to *E. coli* motility. Rather than displaying a non-motile behavior, strains carrying these mutations exhibited an unprecedented hypermotility. This novel hypermotile phenotype was a result of enhanced binding of mutant protein H-NS108I to the flagellar rotor, causing increased flagellar rotational speed.

EXPERIMENTAL PROCEDURES

Bacterial Strains, Plasmids, Phage, Media, and Genetic Techniques—Table I lists all bacterial strains, plasmids, and phage used. Media consisted of Luria-Bertani (LB) broth, LB agar, T broth (1% tryptone, 0.5% NaCl), and soft-agar (T broth, 0.3% agar) (Difco). Antibiotics were added to a final concentration of 100 μg (ampicillin), 20 μg (tetracycline), 20 μg (chloramphenicol), or 50 μg (kanamycin) per ml of medium. Isopropylthiogalactose was used at a final concentration of 1 mM. P1 *vir* generalized transductions were carried out as described previously (29). Cultures were grown at 37 °C for protein purification and 30 °C for motility and flagella assays.

Swarming and Motility—AL127 was transformed with various plasmids. Fresh colonies were picked, inoculated onto low agar (0.3%) tryptone plates, and incubated at 30 °C. Swarm diameters were measured every 2–3 h, beginning 9 h post-inoculation. Differences in motility rates were calculated by comparing the swarm diameter of AL127 expressing an *hns* mutant plasmid relative to the same strain expressing a wild-type *hns* gene, on the same plate for three individual experiments.

Flagellation—Strains were grown at 30 °C overnight in T broth with the appropriate antibiotics and then diluted 25-fold into fresh media and incubated until the A_{600} reached 0.3–0.5. Cells from these cultures were incubated on polylysine-coated coverslips for 15 min at room temperature, rinsed twice with phosphate-buffered saline, and fixed in 3% glutaraldehyde, 0.1 M sodium phosphate buffer (pH 7.4). Bacteria-coated coverslips were dehydrated, critical point dried, attached to aluminum stubs, and sputter coated with gold:palladium. Bacterial flagella were visualized by scanning electron microscopy (Cambridge Stereo Scan S200, LEO Electron Microscopy, Inc.). Flagella were counted on at least 10 fields per strain.

Tethering Experiments—Tethering for the flagellar rotational bias and speed experiments was performed as described previously (30), with the following modifications: diluted cultures were grown without inducer until the A_{600} reached 0.4–0.8; flagella were sheared with a Tissue Tearor model 985–370 (Biospec Products, Inc.); and a 1:100 dilution of anti-flagella antibody (36) was used. Bacteria were observed by dark field microscopy, recorded to videotape, played back at 1/5 the speed, and scored using The Observer 3.1 videotape analysis system software (Noldus Information Technology). Typically, 30 individual cells were quantitated for 30 s each for CCW bias or 1 min each for

* This work was supported by National Institutes of Health Grant R01 AI34176. The costs of publication of this article were defrayed in part by the payment of page charges. This article must therefore be hereby marked "advertisement" in accordance with 18 U.S.C. Section 1734 solely to indicate this fact.

‡ To whom correspondence should be addressed. Tel.: 919-966-9699; Fax: 919-962-8103; E-mail: kawula@med.unc.edu.

¹ The abbreviations used are: CCW, counterclockwise; CW, clockwise; OD, optical density; PAGE, polyacrylamide gel electrophoresis.

TABLE I
Bacteria, plasmids, and bacteriophage used

	Description	Source
Bacteria		
AL127	RP437 <i>hns2-tetR</i> ; P1 transduction from AL90	This study
AL90	<i>hns2-tetR</i>	Ref. 27
RP437	Wild-type for chemotaxis; <i>thr(Am)-1 leuB6 his-4 metF(Am)159 eda-50 rpsL136 thi-1 ara-14 lacY1 mtl-1 xyl-5 tonA31 tsx-78</i>	Ref. 38
RBB1041	RP437 $\Delta(\textit{cheA-cheZ})::\textit{Zeo}^R$	Gift from Bob Bourret
RP1616	RP437 $\Delta(\textit{cheZ})6725$	Ref. 57
BL21(DE3)	Host strain for His-tagged FliG purification	Novagen
M15(pREP4)	Host strain for His-tagged H-NS purification	Qiagen
Plasmids/Phage		
pMASS46-1	pACYC <i>hnsT108I</i>	This study
pMASS73-4	pACYC <i>hnsA18E</i>	This study
pACYC184	Low-copy cloning vector	New England Biolabs
pTHK116	pBR322 with wild-type <i>hns</i> gene under control of <i>hns-1</i> promoter mutation	Ref. 34
pET28NdefliG	Modification of pETHisG; pET28 with wild-type <i>fliG</i>	Ref. 31
pTHK113	pBR322 <i>hns</i> ⁺	Ref. 34
pQE-60	Cloning vector for C-terminal 6xHis fusions	Qiagen
pDMG1	pQE-60 with wild-type <i>hns</i> from pTHK113	This study
P1	<i>vir</i>	Lab collection

flagellum rotational speed.

Protein Purifications—*E. coli* wild-type H-NS and H-NST108I were each purified as described before (27) except the mutant protein lysate was washed from the double stranded DNA-cellulose column at a lower salt concentration (125 versus 250 mM NaCl) than the wild-type cell lysate. His-tagged FliG was nickel-affinity purified basically by the method of Tokor and Macnab (31) from BL21(DE3) cultures harboring pET28NdefliG. Protein solutions were concentrated with Centricon-10 columns as instructed by the manufacturer (Amicon). Protein concentrations were measured with the Bio-Rad Dc protein assay kit (Bio-Rad).

Fluorescence Anisotropy—H-NS was labeled with the thiol-reactive probe, fluorescein 5-maleimide, after reduction with tris-(2-carboxyethyl)phosphine hydrochloride, according to the manufacturer's instructions (Molecular Probes). Labeled protein was separated from excess probe by G-25 Sephadex protein spin column purification (Boehringer Mannheim). Anisotropy was measured at excitation and emission wavelengths of 490 and 515 nm, respectively. Data was collected on a LS 50B Luminescence Spectrometer with FL Data Manager software (Perkin-Elmer). The K_d was calculated as the FliG concentration corresponding to one-half the maximum anisotropy value on the H-NS-FliG binding curve.

Chemical Cross-linking—FliG was first attached to the heterobifunctional cross-linker, sulfo-succinimidyl-4-(*N*-maleimidomethyl)cyclohexane-1-carboxylate (Pierce) by incubating for 1 h at room temperature. Reactions were quenched by the addition of 1 M Tris (pH 7.5), H-NS (wild-type or T108I) was added, and the entire reaction was incubated another hour. The cross-linking reactions were terminated by the addition of 5× Laemmli denaturing sample buffer. Reactions containing equal amounts of each protein (5 μM) were electrophoresed on a 4–20% denaturing gradient gel (Jule Biotechnologies, Inc.) and visualized by Coomassie or Sypro-Orange (Molecular Probes) staining. Complexes were quantitated by volumetric integration on a Gel-Doc 1000 with Molecular Analyst 2.1 software (Bio-Rad). To ensure that we added equal amounts of wild-type H-NS and H-NST108I to FliG, we also quantitated free, uncomplexed H-NS protein.

Antibody Production and Western Blotting—A C-terminal 6xHis-H-NS fusion protein was expressed from pDMG1 and purified under denaturing conditions according to the manufacturer's instructions (Qiagen). An emulsion of TiterMax (Vaxcel) and 300 μg of 6xHis-H-NS was used to inoculate and boost New Zealand White rabbits. Anti-H-NS antiserum obtained was used at a 1:5000 dilution. Anti-FliG antiserum was kindly provided by David Blair (University of Utah, Salt Lake City, UT) and used at a 1:7000 dilution. H-NS-FliG cross-linked complex reactions were run on 12% SDS-polyacrylamide gel electrophoresis, transferred, probed with antiserum, and detected as described previously (27).

RESULTS

Effect of *hns* Mutations on *E. coli* Motility—H-NS is a global regulator of *E. coli* gene expression (reviewed in Refs. 32 and 33). Mutations in *hns* have pleiotropic effects on the cell altering synthesis of a variety of gene products involved in numerous, diverse biological pathways (24–26). In particular, trans-

poson insertions in *hns* result in the loss of bacterial motility due to the lack of master operon *flhCD* expression (20). We isolated a set of random *hns* mutations² and determined their effect on motility. Plasmids carrying either no insertion (pACYC vector alone), a wild-type *hns* gene (pTHK116), or *hns* point mutations *T108I* (pMASS46-1), or *A18E* (pMASS73-4) were separately introduced into AL127, an *E. coli hns2-tetR* (34) insertion mutant background strain (Table I). Transformants were inoculated onto semi-solid agar plates and motility was determined by measuring the diameter of the bacterial swarm over time. Motility was classified into three distinct categories based on swarm size (Fig. 1). Strains lacking H-NS were non-motile. Motility was restored in these strains upon the addition of a wild-type *hns* clone in *trans*. However, the *hnsT108I* and *hnsA18E* mutations each conferred a greater than 2-fold increase ($2.1 \pm .21$ and $2.5 \pm .17$, respectively) in swarm rate as compared with the wild-type strain. These data represent the first instance in which any *E. coli* mutation, *hns* or otherwise, resulted in a hypermotile phenotype.

Flagellation—H-NS is a positive transcriptional regulator of the *flhCD* operon, the master operon which controls expression of all other flagellar components (1). In the absence of H-NS, flagellar genes are not expressed resulting in the loss of intact flagella and motility (20). One explanation for the hypermotile phenotype that we observed with specific *hns* point mutations was that these alleles affected flagella biosynthesis and/or assembly. To test this hypothesis, we examined strains expressing different *hns* alleles by scanning electron microscopy (SEM). Visually, there was no discernible difference in cell size or shape or flagellum length or distribution between strains carrying a wild-type *hns* allele (Fig. 2A) or either *hns* mutation (Fig. 2, B and C). There was also no statistical difference in the average number of flagella/cell between the control and *hnsA18E* strains and only a very slight increase expressed from the *hnsT108I* allele (Table II). We concluded that the increased motility rates exhibited by the *hnsT108I* and *hnsA18E* alleles were not due to an alteration in the number or construction of functional flagella.

Flagellar Rotational Behavior—*E. coli* swim by rotating their flagella filaments (35, 36) either CCW or CW (7). Motion is an alternating series of smooth runs (CCW rotation) and abrupt directional changes called tumbles (CW rotation) (6). It is possible that the *hnsT108I* and *hnsA18E* mutations caused a shift in flagellar rotational bias resulting in hypermotility.

² G. M. Donato and T. H. Kawula, manuscript in preparation.

Strains bearing *hns* mutant alleles may “run” (*versus* tumble) a higher percentage of the time than their wild-type counterparts. To address this issue, we performed tethering experiments (30) to compare the rotational bias of strains containing wild-type or mutant *hns* genes. In this assay, individual cells harboring plasmid-based *hns* alleles were tethered to a microscope slide via an anti-flagella antibody. The spinning direction of cell bodies was observed and bias was calculated to be the proportion of the time cells spent rotating CCW (Table III).

Wild-type cells generally spin CCW with occasional pauses and direction reversals (36). Both of the wild-type controls (Table III, *lines 1* and *4*) adopted this spinning mode, rotating CCW 85% of the time. Additional controls included a “guttled” strain (RBB1041) which is deleted for the chemotaxis genes and spins only in the default CCW direction (37) (*line 2*), and a CW-biased *cheZ* mutant (RP1616) (38) which only tumbles (*line 3*). Strains with *hns* mutant alleles *T108I* or *A18E* (*lines 5* and *6*) did not favor a higher running (CCW) bias over wild-type

strains. In fact, these strains along with two other *hns* mutations which did not exhibit a hypermotile phenotype (data not shown), tumbled or paused slightly more frequently than wild-type cells (*lines 7* and *8*). Thus, the *hns* mutations did not affect the function of the chemotaxis apparatus or the mechanism of flagellar switching.

Flagellar Speed—Flagella propel bacteria by rotating motor-driven helical filaments (35, 36) whereby swimming speed is directly related to flagellar rotational speed (39). Free-swimming bacteria can transverse 20–60 $\mu\text{m/s}$ in liquid media (40), whereas tethered bacteria can rotate their cell bodies 2–9 revolutions/s (36). We postulated that the *hnsT108I* and *hnsA18E* mutations caused hypermotile bacterial swimming behavior by directly increasing the speed at which individual flagella rotated. Once again, we employed bacterial tethering to measure rotational speed using a host strain (AL128) containing a *cheA-cheZ* deletion as well as an *hns2-tetR* mutation. This strain enabled us to survey cells that were all rotating in one direction, CCW, without the complications of switching. Rotational speed data (Table IV) were accumulated from cells of the same size and tethered at the same point to maintain similar drag coefficients, overall cell geometry, and load. The controls (Table IV, *lines 1* and *2*) displayed similar rotational speeds regardless of the location of *hns* (chromosome- or plasmid-based). In contrast, the addition of either *hns* point mutation in *trans* (*lines 3* and *4*) resulted in significant ($p < .005$ and $p < .025$, respectively) increases in the speed of the tethered cell body. We concluded that *hnsA18E* and *hnsT108I* accelerated flagellar speeds 44–62% (Table IV) over wild-type levels without affecting flagellar assembly (Fig. 2 and Table II) or switching (Table III). This direct effect on flagellum rotational speed likely caused the original swarm plate hypermotile phenotype displayed by these *hns* mutant alleles.

H-NS-FliG Binding via Fluorescence Anisotropy—Flagellar rotation is driven by a reversible rotary motor anchored in the inner membrane at the base of the flagellum (reviewed in Refs. 1 and 3). The motor consists of a stator (MotA and MotB) and a rotor (FliG, FliM, and FliN). The three rotor proteins interact

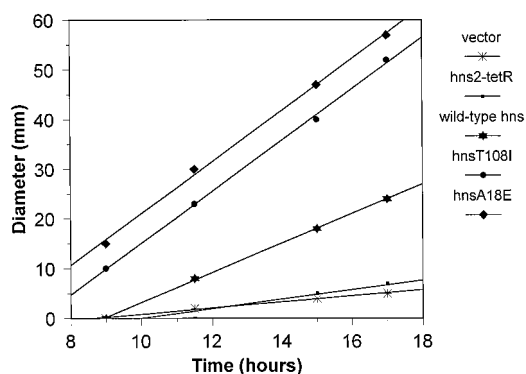


FIG. 1. **Swarm plate assay.** Fresh colonies from strains carrying the indicated alleles were inoculated onto semi-solid agar plates and grown at 30 °C. Growth was measured as the diameter of the bacterial swarm over several time points. Bacteria with swarm diameters under 10 mm at the end of 17 h incubation were considered non-motile. Data representative of three individual experiments. *, vector; ■, *hns2-tetR*; ★, wild-type *hns*; ●, *hnsT108I*; ◆, *hnsA18E*.

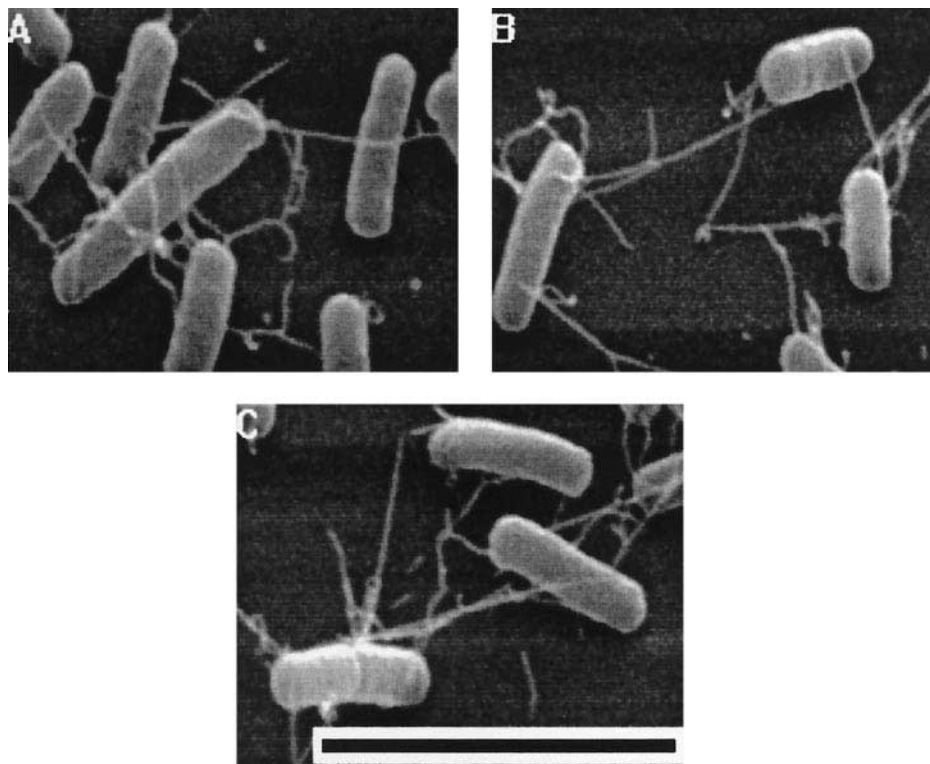


FIG. 2. **Scanning electron micrographs.** AL127 (*hns2-tetR*) carrying (A) wild-type *hns* (pTHK116), (B) *hnsT108I* (pMASS46-1), or (C) *hnsA18E* (pMASS73-4). Magnification, $\times 5000$; scale bar, 10 μm .

TABLE II
Quantitation of bacterial flagellation

Strain Name	Plasmid ^a		Number flagella/cell ^b
	Name	Description	
AL127 (<i>hns2-tetR</i>)	pTHK116	Wild-type <i>hns</i>	3.1
AL127	pMASS46-1	<i>hnsT108I</i>	3.8
AL127	pMASS73-4	<i>hnsA18E</i>	3.1

^a In all plasmids *hns* gene driven by *hns-1* promoter point mutation (34). pTHK116 carries wild-type *hns* coding sequence.

^b Flagella on 125–150 cells were counted for each strain.

TABLE III
Determination of flagellar rotational behavior

Strain		Plasmid		Flagellar rotational bias ^a
Name	Description	Name	Description	
				<i>mean ± S.E.</i>
RP437	Wild-type	NA ^b	NA	.85 ± .04
RBB1041	$\Delta(\textit{cheA-cheZ})$	NA	NA	.99 ± .003
RP1616	$\Delta(\textit{cheZ})6725$	NA	NA	0 ± 0
AL127	<i>hns2-tetR</i>	pTHK116	Wild-type <i>hns</i>	.85 ± .03
AL127	<i>hns2-tetR</i>	pMASS46-1	<i>hnsT108I</i>	.60 ± .04
AL127	<i>hns2-tetR</i>	pMASS73-4	<i>hnsA18E</i>	.72 ± .05
AL127	<i>hns2-tetR</i>	pMASS36-1	<i>hnsR93H</i>	.66 ± .03
AL127	<i>hns2-tetR</i>	pMASS49-1	124 Stop	.76 ± .04

^a Bias defined as fraction of time cells rotating CCW. Values can range from 0 (CW only) to 1 (CCW only). Spinning behavior counted for 25–35 cells per strain.

^b NA, not applicable.

TABLE IV
Determination of flagellar rotational speed

Strain		Plasmid		Flagellar rotational speed ^a
Name	Description	Name	Description	
				<i>rpm</i>
RBB1041	$\Delta(\textit{cheA-cheZ})$	NA ^b	NA	268 ± 15
AL128	$\Delta(\textit{cheA-cheZ})$	pTHK116	Wild-type <i>hns</i>	233 ± 19
AL128	$\Delta(\textit{cheA-cheZ})$, <i>hns2-tetR</i>	pMASS46-1	<i>hnsT108I</i>	377 ± 34
AL128	$\Delta(\textit{cheA-cheZ})$, <i>hns2-tetR</i>	pMASS73-4	<i>hnsA18E</i>	335 ± 27

^a Data represent mean ± S.E. of 25–30 cells per strain.

^b NA, not applicable.

with each other (11, 12) to form a switch complex peripherally attached to the inner membrane, facing the cytoplasm (41–43). All three proteins are involved in flagellar assembly, switching, and rotation (13, 14). Since FliG is the motor protein most involved in speed and torque generation (12, 14, 15), we examined the binding between H-NS and FliG in fluorescence anisotropy assays. This technique quantitates protein-protein interactions by measuring the change in anisotropy of a fluorescently labeled protein upon the addition of a second unlabeled protein (44).

Increasing amounts of purified N terminus His-tagged FliG was added to fluorescein-labeled H-NS and emission anisotropy of the fluorophore was assessed (Fig. 3). As the concentration of FliG increased the anisotropy values also increased, reflecting the formation of a slower rotating complex and protein binding. The leveling off of the curve at higher FliG concentrations demonstrated protein binding saturation (45). We calculated the dissociation constant (K_d) for the H-NS-FliG complex to be $2.15 \pm .25 \mu\text{M}$, well within the range of biologically relevant protein associations. These data represent the first direct biochemical evidence that H-NS binds to FliG and forms a complex with the flagellar motor machinery.

H-NS-FliG Binding via Chemical Cross-linking—Since wild-type H-NS bound FliG in the anisotropy studies (Fig. 3), we

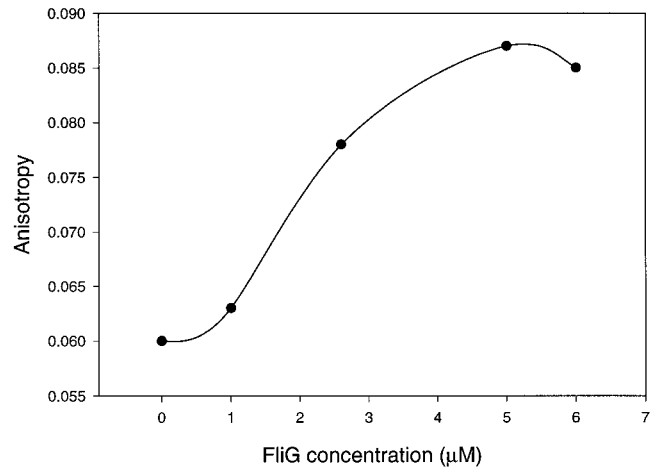


FIG. 3. **Fluorescence anisotropy of H-NS-FliG interactions.** Increasing amounts of FliG were added to fluorescein-labeled H-NS. Ten anisotropy values were measured at each FliG concentration and averaged. Graph is representative of two separate experiments.

wanted to determine if the mutant H-NST108I also bound FliG. A difference in binding affinities between FliG and wild-type or mutant H-NS protein might account for the hypermotile swarm phenotype seen with the mutant. We compared binding capabilities of each of these proteins to FliG by chemical cross-linking.

Equal amounts of either wild-type or T108I H-NS were cross-linked to FliG. H-NS-FliG complexes were trapped, run on SDS-polyacrylamide gels and stained (Fig. 4A). Tandem Western blots were also performed on identical reactions with anti-H-NS (Fig. 4B) and anti-FliG antisera (Fig. 4C) to confirm that the complexes contained both proteins. Several conclusions can be drawn from these results. First, in agreement with previous work (11, 12), FliG self-associated (Fig. 4C) in the absence (*reaction 3*) and presence (*reaction 6*) of cross-linker. Second, both wild-type and T108I H-NS dimerized (Fig. 4A, *reactions 4* and *5*). Also, wild-type H-NS (Fig. 4, A, B, and C, *reaction 7*) and H-NST108I (Fig. 4, A, B, and C, *reaction 8*) each bound to FliG forming a complex of approximately 55 kDa. Furthermore, H-NST108I bound FliG 50% tighter than wild-type H-NS (compare Fig. 4, A-C, *reactions 7* and *8*) at the same protein molar ratios. Although H-NS and FliG obviously bound to each other *in vitro*, this complex did not seem to be the major FliG interaction since most of the protein remained in the monomer form (Fig. 4, A and C, *reactions 7* and *8*). These results demonstrated that the *hnsT108I* mutation conferred an enhanced binding affinity of H-NS for FliG. This increased attachment of H-NST108I to the torque-generating flagellar rotor protein FliG probably accounted for the increased motility rates and flagellum rotational speeds in *E. coli* strains carrying the *hns* mutation.

DISCUSSION

Hypermotility—We studied the effect of two *hns* point mutations, *hnsT108I* and *hnsA18E*, on *E. coli* motility. In swarm plate assays, we observed that each of these *hns* mutations bestowed a hypermotile phenotype (Fig. 1). Swarm rates for strains carrying the *hns* mutant alleles were approximately twice as fast as strains with the wild-type *hns* allele *in trans*. Previously characterized mutations in genes involved in flagella functions have led to three basic mutant phenotype classifications: non-flagellated (Fla⁻) (15), non-rotating flagella (“paralyzed”, Mot⁻) (14), and skewed chemotaxis, either CCW-biased (14) or CW-biased (46). In terms of swarming, mutations typically cause a decrease in motility (47). To the best of our

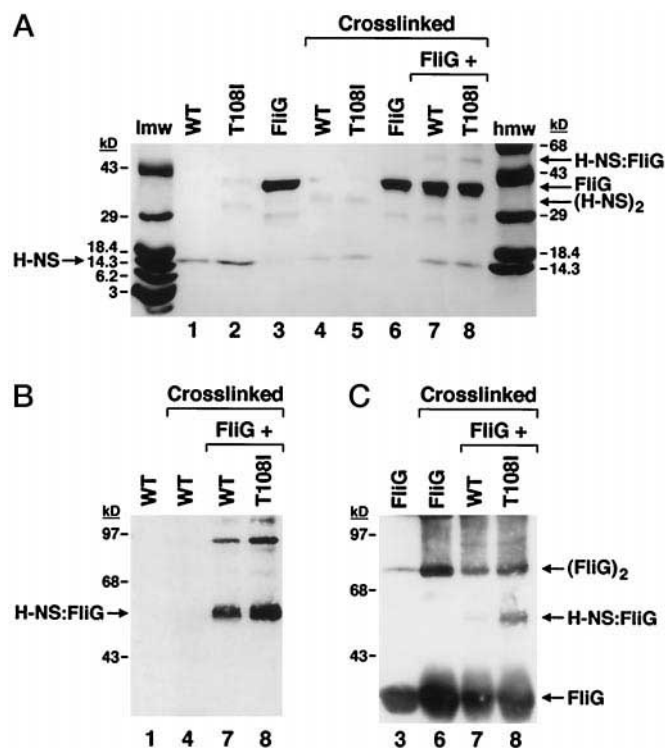


FIG. 4. H-NS-FliG cross-linked complexes. Reactions were incubated at room temperature and equal amounts were electrophoresed on denaturing polyacrylamide gels. A, Coomassie-stained 4–20% SDS-polyacrylamide gradient gel; B, 12% SDS-polyacrylamide gel transferred to nitrocellulose, and probed with H-NS antiserum; C, second half of gel in B probed with FliG antiserum. Protein standard sizes are indicated by lines; *lmw*, low molecular weight markers; *hmw*, high molecular weight markers; protein monomers, dimers, and H-NS-FliG complexes are indicated by arrows. Reactions for all panels: 1, wild-type H-NS only; 2, H-NST108I only; 3, FliG only; 4, wild-type H-NS with cross-linker; 5, H-NST108I with cross-linker; 6, FliG with cross-linker; 7, 1:1 molar ratio of wild-type H-NS to FliG with cross-linker; 8, 1:1 molar ratio of H-NST108I to FliG with cross-linker.

knowledge, *hnsT108I* and *hnsA18E* are the first documented mutations that cause a 2-fold increase in swarm rates.

The mutations studied here represent single H-NS amino acid substitutions of a C-terminal threonine to isoleucine (T108I) and an N-terminal alanine to glutamic acid (A18E). The N-terminal domain of H-NS is ill defined but the C-terminal third of the protein encompasses the DNA-binding domain (48, 49). If H-NSA18E acts by the same mechanism as H-NST108I to increase flagella speed then these mutants may define a FliG-specific binding domain on the H-NS surface. Residues at position 18 and 108 may form a pocket which is near or embodies the actual FliG-binding site. Thus, alterations in these amino acids may enhance FliG binding directly or cause rearrangements in adjacent residues. This possibility suggests that the N and C termini of H-NS are close to each other in the three-dimensional protein structure.

Three ways in which altered H-NS protein could affect motility are by changing the (i) number of flagella assembled, (ii) flagellar directional bias, or (iii) spinning speed of flagella. H-NS is a positive transcriptional activator of the flagellar master operon (20, 50). Thus, it is possible that altered H-NS could be a stronger activator and up-regulate the expression of flagellar structural components. Upon inspection, it was evident that all strains demonstrated the same flagella profile (Fig. 2) and only mutation *hnsT108I* exhibited a minor increase of 0.7 flagella/cell (Table II). We addressed the issue of whether cells bearing the mutant *hns* alleles were running their flagella CCW a longer proportion of time. Regardless of their motility

phenotype, multiple *hns* mutant alleles all displayed similar CCW biases that were not greater than wild-type cells (Table III). Finally, we thought that faster rotating flagella could perhaps account for the increase in swarm motility. In modified tethering assays, we showed that *hnsT108I*- and *hnsA18E*-containing strains did indeed rotate their flagella an average of 53% faster than wild-type cells (Table IV).

H-NS-FliG Interactions—Since our *hns* mutations seemed to be specifically affecting flagellar speed, we investigated the possible interaction between H-NS and the protein complex that controls rotation. Of the three proteins that make up the rotor portion of the motor, we chose to test FliG for the following reasons. First, FliG is situated at the cytoplasmic face of the inner membrane attached to the embedded MS ring through interactions with FliF (41–43). This location allows free access to cytoplasmic H-NS. Second, FliG is presumably part of the active flagellar rotating unit along with the MS ring, rod, hook, and filament (3, 12, 51). Thus, H-NS binding directly to a portion of the moving apparatus could potentially alter speed. Furthermore, FliG functions primarily in flagella rotation and torque generation (12, 14, 15) rather than assembly or switching. Finally, there is previous genetic data indicating that *fliG*- and *hns*-encoded fusion proteins interacted in a yeast two-hybrid system (11).

In our anisotropy studies, it was evident that wild-type H-NS bound FliG, yielding a typical binding curve (Fig. 3). We estimated the K_d to be in the micromolar range, confirming that the H-NS-FliG interaction was significant and biologically relevant. Our data represent the first biochemical evidence to support Marykwas' (11) genetic-based conclusion that H-NS binds to FliG. It also represents the first time H-NS has directly been shown to bind an *E. coli* protein other than itself or homologs. As a modulator of gene expression, H-NS usually functions by binding DNA and exerting an effect on transcription (reviewed in Refs. 32 and 33). It has been suggested by suppressor mutation isolation (52) and co-purification (53) that H-NS may interact with other *E. coli* proteins. However, the only other protein proven to bind H-NS is the bacteriophage T7 gene 5.5 protein product (54).

We carried out cross-linking reactions (Fig. 4) in order to compare the relative binding affinities of FliG for either wild-type H-NS or H-NST108I. We were careful to equalize and monitor H-NS quantities such that any differences in complex intensity were due to binding tightness rather than unequivalent protein concentrations. Each protein dimerized and FliG bound each H-NS species forming 55-kDa heterodimeric complexes, with mutant H-NST108I binding FliG 50% tighter than wild-type H-NS. We are confident that the complexes observed represent an H-NS-FliG interaction since the same overlaid bands were recognized by both anti-H-NS and anti-FliG antiserum (Fig. 4, B and C).

There have been many studies examining the flagellar motor proteins yet H-NS has not been previously found in these complexes. This missing observation may be because non-flagellar components were not assayed for, or the H-NS-FliG binding may be transient, such that, a complex would have to be trapped by a covalent cross-linker rather than pulled down via co-precipitations. The caveat of such a cross-linking experiment is that we are not truly mimicking conditions *in vivo*. In the cell, FliG exists in multiple copies per motor (43) and is known to interact with other proteins such as FliM, FliN, and MotA (12). Therefore, the addition of any of these proteins in our cross-linking assay could alter H-NS-FliG binding mechanisms. Regardless, it seems likely that the hypermotility exhibited by the *hns* mutation is a direct consequence of enhanced binding of H-NST108I to the flagellar rotor protein, FliG.

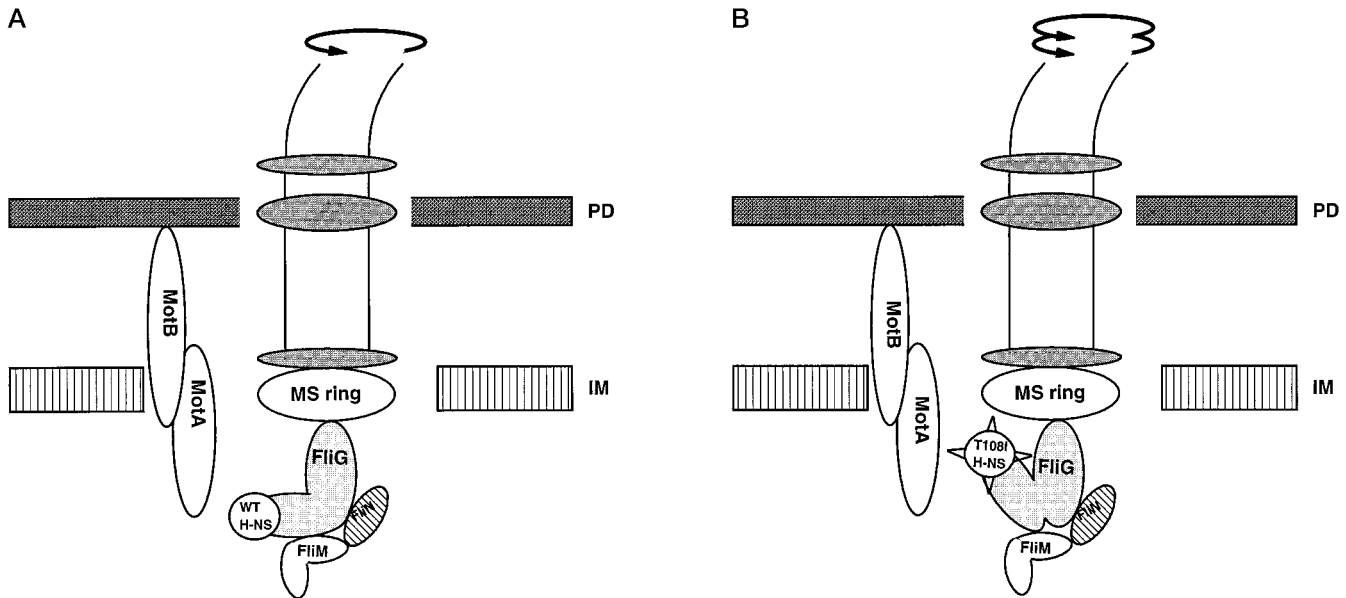


FIG. 5. **Model of H-NS activity at the flagellar rotor.** *A*, wild-type H-NS interactions with FliG; *B*, proposed conformational changes induced by the binding of H-NST108I to FliG. *PD*, peptidoglycan; *IM*, inner membrane. See "Discussion" for details.

Models—No existing model sufficiently accounts for the unexpected effects of H-NS on flagella rotation. Thus, we present a speculative hypothesis of H-NS action (Fig. 5) based on the data presented here as well as previous investigators results (10–12, 31, 41). We postulate that H-NS is involved in torque generation through its interactions with FliG. Given the fact that (i) *hns* mutations resulting in the hypermotile phenotype specifically affected flagellar rotational speed, (ii) speed, torque, and presumably proton-motive force are all directly related (39, 55), and (iii) the C-terminal domain of FliG functions specifically in torque generation (15), we position H-NS at the interface between the rotor and stator, directly linked to the C terminus of FliG (Fig. 5A). Tighter binding of mutant H-NST108I to FliG (Fig. 5B) may cause increases in flagellar speed by altering the conformation of FliG relative to the other rotor proteins and/or the MotA·B complex, thus, compacting the motor complex and allowing faster rotation by creating less friction within the surrounding stationary MotA·B ring complex (56). Alternatively, the movement or rate of proton flux through this channel could also be affected, or the H-NS-FliG complex may play a regulatory role by altering expression of genes downstream of *fliG* in the flagellar assembly cascade.

In totality, this study provides several unique observations about H-NS and *E. coli* motility. We have defined a new swarming mutant class illustrated by a hypermotile phenotype. We have shown that H-NS plays a rare, non-regulatory role in motility. We provided the first biochemical evidence that H-NS binds to the flagellar rotor protein FliG and demonstrated that the tightness of this interaction determines flagellar rotational speed. Future directions will include testing our model in order to provide a suitable mechanistic view of H-NS activity on bacterial motility.

Acknowledgments—We thank David Blair, Bob Macnab, Bob Bourret, Christian Ostermeier, and Sandy Parkinson for strains, plasmids, antiserum, and helpful discussions on bacterial motility. We are especially indebted to the members of the Bourret laboratory for protocols, use of equipment, and their expertise in the field. We gratefully acknowledge the technical assistance of Victoria Madden at the University of North Carolina Microscopy Service Lab, and Marcia Hobbs for production of H-NS antiserum.

REFERENCES

- Macnab, R. M. (1992) *Annu. Rev. Genet.* **26**, 131–158
- Macnab, R. M. (1996) *Escherichia coli and Salmonella typhimurium Cellular and Molecular Biology* (Neidhardt, F. C., Curtiss, R., III, Ingraham, J. L., Lin, E. C. C., Low, K. B., Magasanik, B., Reznikoff, W. S., Riley, M., Schaechter, M., and Umberger, H. E., eds) 2nd Ed., pp. 123–145, American Society for Microbiology, Washington, D. C.
- Blair, D. F. (1995) *Annu. Rev. Microbiol.* **49**, 489–522
- Larsen, S. H., Adler, J., Gargus, J. J., and Hogg, R. W. (1974) *Proc. Natl. Acad. Sci. U. S. A.* **71**, 1239–1243
- Manson, M. D., Tedesco, P., Berg, H. C., Harold, F. M., and van der Drift, C. (1977) *Proc. Natl. Acad. Sci. U. S. A.* **74**, 3060–3064
- Berg, H. C., and Brown, D. A. (1972) *Nature* **239**, 500–504
- Larsen, S. H., Reader, R. W., Kort, E. N., Tso, W.-W., and Adler, J. (1974) *Nature* **249**, 74–77
- Blair, D. F., and Berg, H. C. (1990) *Cell* **60**, 439–449
- Blair, D. F., and Berg, H. C. (1991) *J. Mol. Biol.* **221**, 1433–1442
- Garza, A. G., Harris-Haller, L. W., Stoebner, R. A., and Manson, M. D. (1995) *Proc. Natl. Acad. Sci. U. S. A.* **92**, 1970–1974
- Marykwas, D. L., Schmidt, S. A., and Berg, H. C. (1996) *J. Mol. Biol.* **256**, 564–576
- Tang, H., Braun, T. F., and Blair, D. F. (1996) *J. Mol. Biol.* **261**, 209–221
- Yamaguchi, S., Fujita, H., Ishihara, A., Aizawa, S.-I., and Macnab, R. M. (1986) *J. Bacteriol.* **166**, 187–193
- Irikura, V. M., Kihara, M., Yamaguchi, S., Sockett, H., and Macnab, R. M. (1993) *J. Bacteriol.* **175**, 802–810
- Lloyd, S. A., Tang, H., Wang, X., Billings, S., and Blair, D. F. (1996) *J. Bacteriol.* **178**, 223–231
- Welch, M., Oosawa, K., Aizawa, S.-I., and Eisenbach, M. (1993) *Proc. Natl. Acad. Sci. U. S. A.* **90**, 8787–8791
- Vogler, A. P., Homma, M., Irikura, V. M., and Macnab, R. M. (1991) *J. Bacteriol.* **173**, 3564–3572
- Tang, H., Billings, S., Wang, X., Sharp, L., and Blair, D. F. (1995) *J. Bacteriol.* **177**, 3496–3503
- Hinton, J. C. D., Santos, D. S., Seirafi, A., Hulton, C. S. J., Pavitt, G. D., and Higgins, C. F. (1992) *Mol. Microbiol.* **6**, 2327–2337
- Bertin, P., Terao, E., Lee, E. H., Lejeune, P., Colson, C., Danchin, A., and Collatz, E. (1994) *J. Bacteriol.* **176**, 5537–5540
- Spassky, A., Rimsky, S., Garreau, H., and Buc, H. (1984) *Nucleic Acids Res.* **12**, 5321–5340
- Falconi, M., Gualtieri, M. T., LaTeana, A., Losso, M. A., and Pon, C. L. (1988) *Mol. Microbiol.* **2**, 323–329
- May, G., Dersch, P., Haardt, M., Middendorf, A., and Bremer, E. (1990) *Mol. Gen. Genet.* **224**, 81–90
- Bertin, P., Lejeune, P., Laurent-Winter, C., and Danchin, A. (1990) *Biochimie (Paris)* **72**, 889–891
- Yamada, H., Yoshida, T., Tanaka, K., Sasakawa, C., and Mizuno, T. (1991) *Mol. Gen. Genet.* **230**, 332–336
- Laurent-Winter, C., Ngo, S., Danchin, A., and Bertin, P. (1997) *Eur. J. Biochem.* **244**, 767–773
- Donato, G. M., Lelivelt, M. J., and Kawula, T. H. (1997) *J. Bacteriol.* **179**, 6618–6625
- Ueguchi, C., and Mizuno, T. (1993) *EMBO J.* **12**, 1039–1046
- Miller, J. H. (1972) *Experiments in Molecular Genetics*, Cold Spring Harbor Laboratory, Cold Spring Harbor, NY
- Bray, D., Bourret, R. B., and Simon, M. I. (1993) *Mol. Biol. Cell* **4**, 469–482
- Toker, A. S., and Macnab, R. M. (1997) *J. Mol. Biol.* **273**, 623–634
- Ussery, D. W., Hinton, J. C. D., Jordi, B. J. A. M., Granum, P. E., Seirafi, A., Stephen, R. J., Tupper, A. E., Berridge, G., Sidebotham, J. M., and Higgins, C. F. (1994) *Biochimie (Paris)* **76**, 968–980
- Altung, T., and Ingmer, H. (1997) *Mol. Microbiol.* **24**, 7–17
- Kawula, T. H., and Orndorff, P. E. (1991) *J. Bacteriol.* **173**, 4116–4123

35. Berg, H. C., and Anderson, R. A. (1973) *Nature* **245**, 386–382
36. Silverman, M., and Simon, M. (1974) *Nature* **249**, 73–74
37. Conley, M. P., Wolfe, A. J., Blair, D. F., and Berg, H. C. (1989) *J. Bacteriol.* **171**, 5190–5193
38. Parkinson, J. S. (1978) *J. Bacteriol.* **135**, 45–53
39. Jones, C. J., and Aizawa, S.-I. (1991) *Adv. Microbial Physiol.* **32**, 109–172
40. Macnab, R. M., and Aizawa, S.-I. (1984) *Annu. Rev. Biophys. Bioeng.* **13**, 51–83
41. Francis, N. R., Irikura, V. M., Yamaguchi, S., DeRosier, D. J., and Macnab, R. M. (1992) *Proc. Natl. Acad. Sci. U. S. A.* **89**, 6304–6308
42. Oosawa, K., Ueno, T., and Aizawa, S.-I. (1994) *J. Bacteriol.* **176**, 3683–3691
43. Zhao, R., Amsler, C. D., Matsumura, P., and Khan, S. (1996) *J. Bacteriol.* **178**, 258–265
44. Lakowicz, J. R. (1983) *Principles of Fluorescence Spectroscopy*, Plenum Press, New York
45. Kersten, S., Kelleher, D., Chambon, P., Gronemeyer, H., and Noy, N. (1995) *Proc. Natl. Acad. Sci. U. S. A.* **92**, 8645–8649
46. Togashi, F., Yamaguchi, S., Kihara, M., Aizawa, S.-I., and Macnab, R. M. (1997) *J. Bacteriol.* **179**, 2994–3003
47. Lloyd, S. A., and Blair, D. F. (1997) *J. Mol. Biol.* **266**, 733–744
48. Ueguchi, C., Suzuki, T., Yoshida, T., Tanaka, K., and Mizuno, T. (1996) *J. Mol. Biol.* **263**, 149–162
49. Shindo, H., Iwaki, T., Ieda, R., Kurumizaka, H., Ueguchi, C., Mizuno, T., Morikawa, S., Nakamura, H., and Kuboniwa, H. (1995) *FEBS Lett.* **360**, 125–131
50. Kutsukake, K. (1997) *Mol. Gen. Genet.* **254**, 440–448
51. Harshey, R. M., and Toguchi, A. (1996) *Trends Microbiol.* **4**, 226–231
52. Kawula, T. H., and Lelivelt, M. J. (1994) *J. Bacteriol.* **176**, 610–619
53. Kajitani, M., and Ishihama, A. (1991) *Nucleic Acids Res.* **19**, 1063–1066
54. Liu, Q., and Richardson, C. C. (1993) *Proc. Natl. Acad. Sci. U. S. A.* **90**, 1761–1765
55. Amsler, C. D., Cho, M., and Matsumura, P. (1993) *J. Bacteriol.* **175**, 6238–6244
56. Khan, S., Dapice, M., and Reese, T. S. (1988) *J. Mol. Biol.* **202**, 575–584
57. Liu, J., and Parkinson, J. S. (1989) *Proc. Natl. Acad. Sci. U. S. A.* **86**, 8703–8707